J|A|C|S
ARTICLES
Published on Web 12/15/2001

Computational Assessment of the Electronic Structures of Cyclohexa-1,2,4-triene, 1-Oxacyclohexa-2,3,5-triene (3δ^2-Pyran), Their Benzo Derivatives, and Cyclohexa-1,2-diene. An Experimental Approach to 3δ^2-Pyran§

Bernd Engels,* Jan C. Schöneboom, Arno F. Münster,*,† Stefan Groetsch, and Manfred Christl*

Contribution from the Institut für Organische Chemie and Institut für Physikalische Chemie, Universität Würzburg, Am Hubland, D-97074 Würzburg, Germany

Received May 17, 2001. Revised Manuscript Received September 17, 2001

Abstract: The six-membered cyclic allenes given in the title have been studied theoretically by means of an MR-CI approach. For all compounds, the allene structures were found to be the ground states in the gas phase. In the cases of cyclohexa-1,2-diene (**1**), the isobenzene **2**, and the isonaphthalene **7**, the most stable structures having a planar allene moiety are the diradicals **1b**, **2b**, and **7b**, representing the transition states for the racemization of **1a**, **2a**, and **7a** and being less stable than the latter by 14.1, 8.9, and 11.2 kcal/mol, respectively. At variance with this order, the 3δ^2-pyran **4** and the chromene **5** have the zwitterions **4c** and **5c** as the most stable planar structures, which lie only 1.0 and 5.4 kcal/mol above **4a** and **5a**, respectively. According to the simulation of the solvent effect, **4c** even becomes the ground state of **4** in THF solution. The frontier orbitals of the respective states of **2** and **4** suggest different rates and sites for the reaction with nucleophiles. For the first time, the pyran **4** has been generated and trapped. As a precursor for **4**, 3-bromo-4*H*-pyran (**9**) was chosen, the synthesis of which was achieved on two routes from 4*H*-pyran. The treatment of **9** with potassium *tert*-butoxide (KO*t*-Bu)/18-crown-6 gave 4-*tert*-butoxy-4*H*-pyran as the only discernible product, whether styrene or furan was present, indicating the interception of **4** by KO*t*-Bu. Finally, the disagreement between the experiment and the theory concerning the heat of formation and the electronic nature of the isobenzene **2** is resolved by demonstrating that the experimental data can provide only an upper limit of the $\Delta H_f°$ value.

1. Introduction

Cyclohexa-1,2-diene (**1**) and a number of its simple derivatives are extremely short-lived intermediates,[1,2] which can be directly observed at best by IR spectroscopy in a matrix at low temperatures[3,4] or by photoelectron spectroscopy in the gas phase[5] after generation from a suitable precursor by flash vacuum pyrolysis or photolysis. Stable compounds result only if several atoms of a second-row element of the periodic table such as silicon[6] or phosphorus[7] are members of the tether connecting the termini of the allene moiety.

Much attention has recently been dedicated to cyclohexa-1,2,4-triene, the isobenzene **2**. For a number of years, derivatives of **2** have been considered to be initially formed as Diels−Alder adducts in reactions of vinylacetylenes with acetylenes.[1,8] Furthermore, two rearrangement reactions are believed to proceed via derivatives of **2**.[9] Conclusive evidence for the parent isobenzene **2** was obtained by the isolation of trapping products, after **2** had been generated in the presence of activated olefins. As methods of generation, the Doering−Moore−Skattebøl reaction of 6,6-dihalobicyclo[3.1.0.]hexenes,[10] the electrocyclization of hexa-1,3-dien-5-yne,[11] and the β-elimination of hydrogen bromide from 1-bromocyclohexa-1,4-diene[12] were

* Address correspondence regarding the calculations to B.E., the simulation of the kinetic data to A.F.M., and the experiments to M.C.

† Institut für Physikalische Chemie.

§ Cycloallenes. Part 17. For part 16, see: Drinkuth, S.; Groetsch, S.; Peters, E.-M.; Peters, K.; Christl, M. *Eur. J. Org. Chem.* **2001**, 2665-2670.

(1) Johnson, R. P. *Chem. Rev.* **1989**, *89*, 1111−1124.
(2) Balci, M.; Taskesenligil, Y. *Adv. Strained Interesting Org. Mol.* **2000**, *8*, 43−81.
(3) Cyclohexa-1,2-diene (**1**): (a) IR absorption at 1865 cm^{-1}: Wentrup, C.; Gross, G.; Maquestiau, A.; Flammang, R. *Angew. Chem., Int. Ed. Engl.* **1983**, *22*, 542. (b) IR absorption at 1829 cm^{-1}: Runge, A.; Sander, W. *Tetrahedron Lett.* **1986**, *27*, 5835−5838. (c) The repetition of the flash vacuum thermolysis of the ketene taken as precursor for **1** in ref 3a did not yield a product with an IR absorption at 1865 cm^{-1}, whereas the IR absorption of ref 3b was shown to be due to trimethylstannane: Sierakowski, C. Dissertation, Justus-Liebig-Universität Gieβen, 1991. We are grateful to Professor Günther Maier for drawing our attention to these results.
(4) 2-Chloro-3δ^2-chromene (**6**): Khasanova, T.; Sheridan, R. S. *J. Am. Chem. Soc.* **2000**, *122*, 8585−8586.
(5) Werstiuk, N. H.; Roy, C. D.; Ma, J. *Can. J. Chem.* **1996**, *74*, 1903−1905.
(6) Pang, Y.; Petrich, S. A.; Young, V. G., Jr.; Gordon, M. S.; Barton, T. J. *J. Am. Chem. Soc.* **1993**, *115*, 2534−2536. Shimizu, T.; Hojo, F.; Ando, W. *J. Am. Chem. Soc.* **1993**, *115*, 3111−3115.
(7) Hofmann, M. A.; Bergsträβer, U.; Reiβ, G. J.; Nyulászi, L.; Regitz, M. *Angew. Chem., Int. Ed.* **2000**, *39*, 1261−1263.
(8) Danheiser, R. L.; Gould, A. E.; de la Pradilla, R. F.; Helgason, A. L. *J. Org. Chem.* **1994**, *59*, 5514−5515. Burrell, R. C.; Daoust, K. J.; Bradley, A. Z.; DiRico, K. J.; Johnson, R. P. *J. Am. Chem. Soc.* **1996**, *118*, 4218−4219. Gevorgyan, V.; Takeda, A.; Homma, M.; Sadayori, N.; Radhakrishnan, U.; Yamamoto, Y. *J. Am. Chem. Soc.* **1999**, *121*, 6391−6402.
(9) van Loon, J.-D.; Seiler, P.; Diederich, F. *Angew. Chem., Int. Ed. Engl.* **1993**, *32*, 1706. Freeman, P. K.; Pugh, J. K. *J. Org. Chem.* **1999**, *64*, 3947−3953.

Chart 1

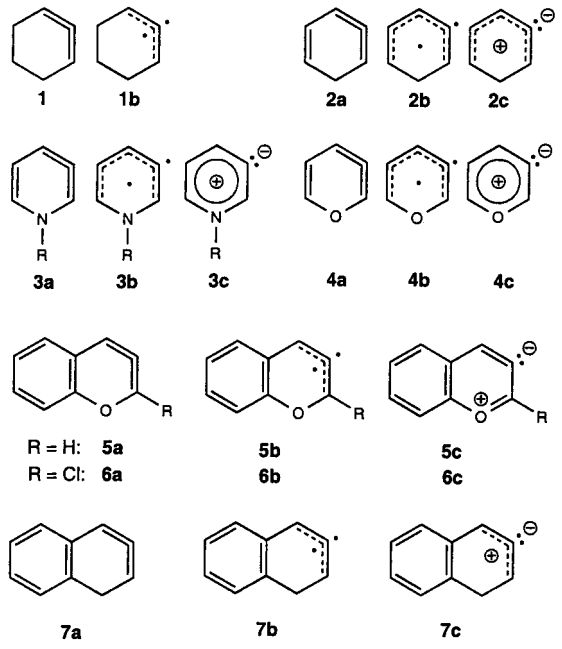

successful. From a kinetic investigation using the second method in the presence of triplet oxygen ($^3O_2$), Roth et al.[13] deduced that the heat of formation ($\Delta H_f°$) of **2** is 85 kcal/mol greater than that of benzene. By comparison with the value estimated from group equivalents, they assumed that **2** is more likely to have the diradical nature **2b** than the allene structure **2a** (Chart 1). However, high-level quantum chemical calculations disagreed with this $\Delta H_f°$ value and, moreover, invariably ascribed the allene structure **2a** to the species.[14−16]

Shevlin at al.[17a] have postulated 3δ^2-pyridines (**3**), the 6-aza derivatives of **2**, as intermediates in the reaction cascades that follow the addition of carbon atoms to pyrroles. The possible intervention of a benzo derivative of **3** has recently been described by Frey et al.[17b] On the basis of the observed products and preliminary quantum chemical calculations, Shevlin et al.[17a] favor the dipolar structure **3c** over the allene structure **3a** and do not comment on the diradical alternative **3b** (Chart 1). The attempt to generate 3δ^2-pyran (**4**) analogously to **3**, that is, by addition of a carbon atom onto furan, failed, however.[18] Derivatives of **4** have been assumed to be initially formed as intramolecular Diels−Alder adducts of diynediones.[19] Khasanova and Sheridan[4] have recently published an experimental and theoretical study of 2-chloro-3δ^2-chromene (**6**). The species was

Scheme 1

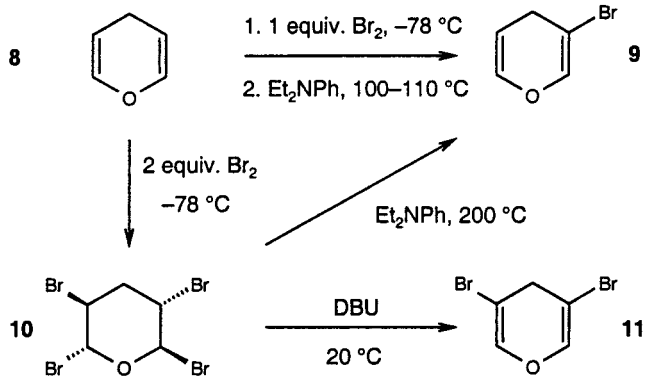

calculated to have the allene ground state **6a** with the zwitterion **6c** being higher in energy by only 2.5 kcal/mol and serving as the transition structure for the enantiomerization of **6a** (Chart 1).

Herein, we present the generation of **4** by the β-elimination route. The reactivity of **4** proved to be rather astounding, in particular when compared to that of its benzo derivative **5**.[20] In consequence, we have tried to computationally assess the electronic structure of **4** and **5** to answer the question of whether these intermediates are genuine allenes (**4a**, **5a**) or diradicals (**4b**, **5b**) or zwitterions (**4c**, **5c**) (Chart 1). The energetics of the carbocyclic analogues of **4** and **5**, that is, **2** and the isonaphthalene **7**, were also computed to examine the influence of the oxygen atom as compared to that of a methylene group. A further target of the calculations was **1**, the parent of the six-membered cyclic allenes. Since the understanding of the effect of the oxygen atom on the reactivity on going from **2** and **7** to **4** and **5** requires the knowledge of the nature of the low-lying excited states, these were calculated as well. The results explain the differences between the chemical behavior of the various cyclic allenes.

The final topic of our study is the above-mentioned disagreement regarding the nature of **2** between the conclusion based on experimental findings by Roth et al.[13] and high-level quantum chemical calculations. To ensure that our approach provides a satisfactory description of six-membered cyclic allenes, we reexamined the underlying assumption necessary for the interpretation of the experiments.[13] Proposing an alternative assumption and newly simulating the rate data, we could resolve the discrepancy between experiment and theory.

2. Generation and Interception of 3δ^2-Pyran (4)

Following the β-elimination strategy,[1,2] we chose 3-bromo-4*H*-pyran (**9**) as a precursor for **4** and prepared **9** from 4*H*-pyran (**8**) by addition of 1 equiv of bromine and heating of the product without isolation with *N*,*N*-diethylaniline (Scheme 1). Since some **8** was regenerated by reductive elimination,[21] the yield of **9** was only 11%. A second access to **9** was found in the treatment of the tetrabromide **10**, isolated in 63% yield after addition of 2 equiv of bromine to **8**, with *N*,*N*-diethylaniline at 200 °C (Scheme 1). In addition to **9** (19% yield), this reaction gave rise to some **8** again. By employing 1,8-diazabicyclo[5.4.0]-undec-7-ene (DBU) as base for the elimination, we obtained 3,5-dibromo-4*H*-pyran (**11**) in 0.3% yield (Scheme 1). In

(10) Christl, M.; Braun, M. In *Strain and Its Implications in Organic Chemistry*; de Meijere, A., Blechert, S., Eds.; Kluwer: Dordrecht, 1989; pp 121−131. Christl, M.; Braun, M.; Müller, G. *Angew. Chem., Int. Ed. Engl.* **1992**, *31*, 473−476.
(11) Hopf, H.; Berger, H.; Zimmermann, G.; Nüchter, U.; Jones, P. G.; Dix, I. *Angew. Chem., Int. Ed. Engl.* **1997**, *36*, 1187−1190.
(12) Christl, M.; Groetsch, S. *Eur. J. Org. Chem.* **2000**, 1871−1874.
(13) Roth, W. R.; Hopf, H.; Horn, C. *Chem. Ber.* **1994**, *127*, 1765−1779.
(14) Janoscheck, R. *Angew. Chem., Int. Ed. Engl.* **1992**, *31*, 476−478.
(15) Bettinger, H. F.; Schreiner, P. R.; Schaefer, H. F., III; Schleyer, P. v. R. *J. Am. Chem. Soc.* **1998**, *120*, 5741−5750.
(16) Li, Z.; Rogers, D. W.; McLafferty, F. J.; Mandziuk, M.; Podosenin, A. W. *J. Phys. Chem. A* **1999**, *103*, 426−430.
(17) (a) Emanuel, C. J.; Shevlin, P. B. *J. Am. Chem. Soc.* **1994**, *116*, 5991−5992. Pan, W.; Shevlin, P. B. *J. Am. Chem. Soc.* **1997**, *119*, 5091−5094. (b) Frey, L. F.; Tillyer, R. D.; Ouellet, S. G.; Reamer, R. A.; Grabowski, E. J. J.; Reider, P. J. *J. Am. Chem. Soc.* **2000**, *122*, 1215−1216.
(18) Dyer, S. F.; Shevlin, P. B. *J. Am. Chem. Soc.* **1979**, *101*, 1303−1304. Pan, W.; Balci, M.; Shevlin, P. B. *J. Am. Chem. Soc.* **1997**, *119*, 5035−5036.
(19) Wills, M. S. B.; Danheiser, R. L. *J. Am. Chem. Soc.* **1998**, *120*, 9378−9379.
(20) Christl, M.; Drinkuth, S. *Eur. J. Org. Chem.* **1998**, 237−241.
(21) Caubère, P. *Chem. Rev.* **1993**, *93*, 2317−2334.

Scheme 2

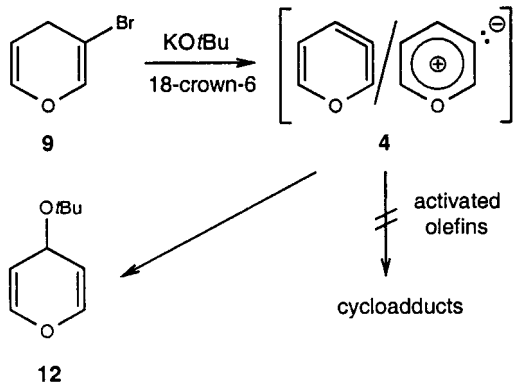

contrast to **8** and **9**, the tetrabromide **10** is a stable compound and thus is useful as a storable precursor of **9**.

It turned out that **9**, dissolved in furan or styrene, did not react with potassium *tert*-butoxide (KO*t*-Bu). The low acidity of the methylene group of **9** may be caused by the antiaromatic nature of the anion resulting on deprotonation. On addition of 18-crown-6 to the reaction mixtures, **9** was consumed, but no products were observed that could have formed by cycloaddition of **4** with furan or styrene. The only new compound, also detected as a product of the reaction of **9** dissolved in benzene-d_6 with KO*t*-Bu in the presence of 18-crown-6 and the absence of furan and styrene, was identified to be 4-*tert*-butoxy-4*H*-pyran (**12**) (Scheme 2). The lability of **12** prevented its isolation, but a high-resolution mass spectrum and the NMR spectra leave no doubt as to its structure. Particularly indicative are the signals of an AA′MM′X system at δ 6.60 (H2, H6), 5.01 (H3, H5), and 4.52 (H4) in the ^{1}H NMR spectrum in $CDCl_3$ (see Supporting Information).

Efficient cycloadditions with activated olefins are a feature of cyclohexa-1,2-diene (**1**) and most of its known derivatives,[1,2] among them **2**,[10−12] **5**,[20] and **7**.[10,22] Cycloadducts of **4** with furan and styrene should be stable enough for direct observation. Thus, their absence as well as the formation of **12** indicate the special character of **4**. Nucleophiles attack unpolar six-membered cyclic allenes such as **1**,[1] **7**,[22] and its 1,1-dimethyl derivative[23] at the central allene carbon atom exclusively. However, the dihydro derivative of **4**, the unsymmetrical isopyran, reacts at all three allene carbon atoms with KO*t*-Bu[24] and at the central or one terminal allene carbon atom with enolates.[25] The involvement of the allene termini has been interpreted as indication of a polarization of this cyclic allene in terms of a zwitterionic structure.[20] That **5** takes up KO*t*-Bu exclusively at the allene terminus bearing the oxygen atom, giving rise to an acetal, is evidence for an even greater contribution of the zwitterion **5c** to the ground state of **5**. Yet, if furan or styrene is present, **5** prefers to undergo cycloaddition.[20] This reactivity order could be reversed in the case of **4**, that is, **4** might favor nucleophiles over activated olefins since the polar character of **4** should be enhanced relative to that of **5** because of the greater gain in aromatic stabilization energy on conversion of the allene **4a** into the dipole **4c** as compared to that of **5a** into **5c**. Since pyrylium ions are attacked by nucleophiles in position 2, 4, or 6,[26] the ether **12** provides experimental evidence for the strong polar nature of the ground state of **4** (Scheme 2), which is in line with the results of the calculations presented below. A product derived from the reaction of KO*t*-Bu with **4** at the centers bearing the oxygen atom was not detected, which may be explained by the instability of such a compound. As a 2*H*-pyran, the possibly formed acetal could have undergone an electrocyclic ring opening,[27] and the resulting aldehyde might have been subject to further reactions. Indeed, the ^{1}H NMR spectra of the mixtures containing **12** display aldehyde signals of substantial intensity (see Supporting Information).

3. Computational Details

For a reliable description of systems which possess diradical character, a multireference treatment is essential in most cases. Since the planar diradical species appeared to be important for the understanding of the chemistry of cyclic allenes, MR-CI+Q and CASPT2 single point energy calculations were employed in the present work. The geometric parameters of the stationary points were optimized using analytical gradients of the complete active space SCF (CASSCF) method and of the density functional theory (DFT). Since the calculated MR-CI+Q energies obtained from the DFT optimized geometries were always slightly lower (0.4−1.0 kcal/mol), we will concentrate on these results. To obtain the minima of a given multiplicity, we performed optimizations without symmetry constraints. The geometric parameters of the different planar singlet species were optimized with C_s symmetry constraints.

For the geometry optimizations, we employed the B88[28a] or B3[28b] exchange expressions in combination with the correlation functionals by Lee, Yang, and Parr (LYP).[29] The unrestricted ansatz was used for all DFT computations (UDFT). The natures of the various stationary points were checked by the number of imaginary frequencies. The DFT approach was also utilized to obtain zero point vibrational energy corrections. The influence of the nuclear motion and temperature effects were incorporated in the standard approach.[30] All DFT calculations as well as (PU)-MP2 and the CCSD(T) single point calculations were performed with the Gaussian 98 program package.[30]

In the CASSCF computations, an eight electron in eight orbital active space ([8,8]-CAS) was used for all species. For the planar structures which possess C_s symmetry, it consists of

(22) Groetsch, S.; Spuziak, J.; Christl, M. *Tetrahedron* **2000**, *56*, 4163−4171.
(23) Miller, B.; Shi, X. *J. Am. Chem. Soc.* **1987**, *109*, 578−579.
(24) Ruzziconi, R.; Naruse, Y.; Schlosser, M. *Tetrahedron* **1991**, *47*, 4603−4610.
(25) Jamart-Grégoire, B.; Grand, V.; Ianelli, S.; Nardelli, M.; Caubère, P. *Tetrahedron Lett.* **1990**, *31*, 7603−7606. Jamart-Grégoire, B.; Mercier-Girardot, S.; Ianelli, S.; Nardelli, M.; Caubère, P. *Tetrahedron* **1995**, *51*, 1973−1984.
(26) Ellis, G. P. In *Comprehensive Heterocyclic Chemistry*, 1st ed.; Katritzky, A. R., Rees, C. W., Boulton, A. J., McKillop, A., Eds.; Pergamon Press: Oxford, 1984; Vol. 3/2b, pp 647−736.
(27) Kuthan, J. *Adv. Heterocycl. Chem.* **1983**, *34*, 145−303. Kuthan, J.; Šebek, P.; Böhm, S. *Adv. Heterocycl. Chem.* **1995**, *62*, 19−135.
(28) (a) Becke, A. D. *Phys. Rev. A: At., Mol., Opt. Phys.* **1988**, *38*, 3098−3100. (b) Becke, A. D. *J. Chem. Phys.* **1993**, *98*, 1372−1377. Becke, A. D. *J. Chem. Phys.* **1993**, *98*, 5648−5652.
(29) Lee, C.; Yang, W.; Parr, R. G. *Phys. Rev. B: Condens. Matter* **1988**, *37*, 785−789.
(30) Frisch, M. J.; Trucks, G. W.; Schlegel, H. B.; Scuseria, G. E.; Robb, M. A.; Cheeseman, J. R.; Zakrzewski, V. G.; Montgomery, J. A., Jr.; Stratmann, R. E.; Burant, J. C.; Dapprich, S.; Millam, J. M.; Daniels, A. D.; Kudin, K. N.; Strain, M. C.; Farkas, O.; Tomasi, J.; Barone, V.; Cossi, M.; Cammi, R.; Mennucci, B.; Pomelli, C.; Adamo, C.; Clifford, S.; Ochterski, J.; Petersson, G. A.; Ayala, P. Y.; Cui, Q.; Morokuma, K.; Malick, D. K.; Rabuck, A. D.; Raghavachari, K.; Foresman, J. B.; Cioslowski, J.; Ortiz, J. V.; Stefanov, B. B.; Liu, G.; Liashenko, A.; Piskorz, P.; Komaromi, I.; Gomperts, R.; Martin, R. L.; Fox, D. J.; Keith, T.; Al-Laham, M. A.; Peng, C. Y.; Nanayakkara, A.; Gonzalez, C.; Challacombe, M.; Gill, P. M. W.; Johnson, B. G.; Chen, W.; Wong, M. W.; Andres, J. L.; Head-Gordon, M.; Replogle, E. S.; Pople, J. A. *Gaussian 98*, revision A.7; Gaussian, Inc.: Pittsburgh, PA, 1998.

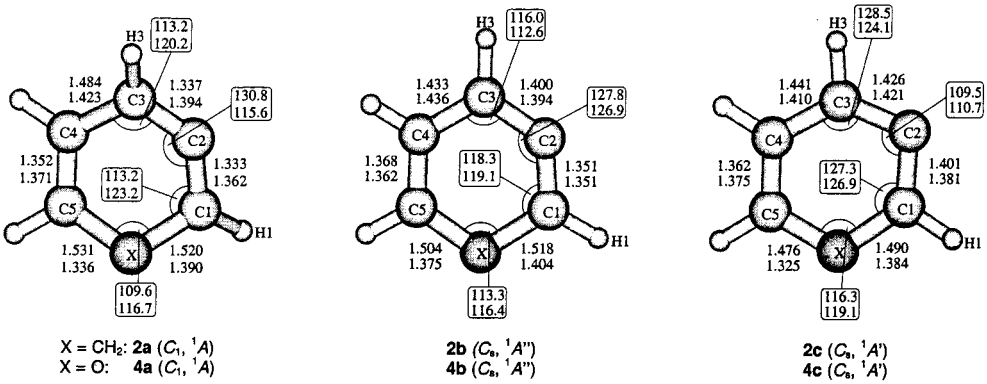

Figure 1. Selected bond lengths (Å) and bond angles (deg) of various stationary points computed (UB3LYP/cc-pVDZ) for the isobenzene **2** (upper values) and the pyran **4** (lower values). Dihedral angles (deg) in **2a**/**4a**: H1−C1−C2−C3, 146.4/170.4; H3−C3−C2−C1, 145.8/164.0; X−C1−C2−C3, −16.2/−10.9; C1−C2−C3−C4, −18.2/−11.2.

a [4,4] space for A' and a [4,4] space for A'' in the case of the monocycles and a [2,2] space for A' and a [6,6] space for A'' in the case of the benzannulated systems. The A'' part encloses the π orbitals, while the A' space includes the σ orbitals. The CASPT2 single point energy calculations utilized the [8,8]-CASSCF wave functions as reference. The CASSCF as well as the CASPT2 calculations were performed with the MOLCAS program package.[31]

The MR-CI approach used in this study is an individually selecting multireference CISD algorithm.[32] The reference spaces consisted of up to seven configurations, leading to MR-CI configuration spaces of up to 93 million configuration state functions (CSFs). The secular equations solved were in the order of nine million CSFs. The influence of the neglected CSFs was estimated by the Buenker-Peyerimhoff extrapolation scheme.[33,34] For the MR-CI treatment, the [8,8]-CASSCF orbitals were used. The influence of higher excitations was estimated by the normalized form of the usual Davidson correction.[35] In the following, these calculations are abbreviated as MR-CI+Q. All MR-CI computations were performed with the DIESEL-MRCI program package.[36] The ΔG_{298} values were computed by adding the thermal corrections from DFT (UB3LYP/cc-pVDZ) frequency calculations to the electronic energies from MR-CI+Q/cc-pVDZ single point calculations.

For the CASPT2 and the MR-CI calculations, we employed the cc-pVDZ[37] and the ANO-l basis set[38] in the (14s9p4d) → [5s3p1d] and (8s4p) → [3s1p] contraction for the heavier and the hydrogen atoms, respectively. While the cc-pVDZ basis is of valence double-ζ quality, the ANO-l basis has a valence triple-ζ quality. Geometry optimizations were performed with the cc-pVDZ basis set given by Dunning.[37]

To simulate solvent effects, we utilized the polarizable conductor calculation model (CPCM)[39] as implemented in Gaussian 98. We simulated THF as the solvent employing a dielectric constant of 7.58. Geometry optimizations in the presence of the simulated solvent were carried out at the UB3LYP/6-31+G(d) level. The obtained free energies of solvation were used as a correction term to the MR-CI+Q/cc-pVDZ values of the free energy in the gas phase.

While a multireference ansatz is necessary for an accurate computation of the energetics, a qualitative description of the electron density distribution can already be obtained on the basis of less sophisticated treatments. This can be seen from the orbitals furnished by CASSCF calculations, which do not differ significantly from those obtained from the UDFT approach. This shows that the electron density distributions provided by the various treatments are qualitatively equal. Consequently, the Natural Resonance Theory (NRT)[40] analysis based on the DFT result is employed to obtain qualitative insights into electron density distributions.

4. Results of the Calculations of 1, 2, 4, 5, and 7 and Chemical Implications

Isobenzene 2 and Isonaphthalene 7. The allene structures and the planar species were examined. For the latter, we also computed the first excited singlet and the lowest lying triplet states. The geometric parameters of these stationary points are depicted in Figures 1 and 2. Figures 3 and 4 summarize the calculated relative ΔG_{298} values. Table 1 contains the relative electronic energies for several stationary points of **2** at various levels of theory. The results of the NRT analysis and the coefficients of the dominating configurations of the MR-CI wave functions are given in Tables 2 and 3.

In accordance with previous computations[14−16] for **2**, our calculations predict a C_1-symmetric structure (allene geometry **2a**, Chart 1) to be the energy minimum. The bond distances (Figure 1) at the allene subunit (C1−C2, 1.333 Å; C2−C3, 1.337 Å) indicate a considerable double bond character, although the structure is found to be highly strained, as can be seen from the angle C1−C2−C3 (130.8°). The dihedral angles at the allene subunit are calculated to be about −16.2 and −18.2° within the ring (C1−C2−C3−C4, CH_2−C1−C2−C3) and 146.4 and 145.8° if the hydrogen atoms are involved (H1−C1−C2−C3,

(31) Anderson, K.; Blomberg, M. R. A.; Fülcher, M. P.; Karlström, G.; Lindh, R.; Malmqvist, P. Å.; Neogrády, P.; Olsen, J.; Roos, B. O.; Sadley, A. J.; Schütz, M.; Seijo, L.; Serrano-Andrés, L.; Siegbahn, P. E. M.; Widmark, P.-O. *MOLCAS*, version 4; University of Lund: Sweden, 1997.
(32) Hanrath, M.; Engels, B. *Chem. Phys.* **1997**, *225*, 197−202.
(33) Buenker, R. J.; Peyerimhoff, S. D. *Theor. Chim. Acta* **1974**, *35*, 33−58.
(34) Buenker, R. J.; Peyerimhoff, S. D. *Theor. Chim. Acta* **1975**, *39*, 217−228.
(35) Langhoff, S. R.; Davison, E. R. *Int. J. Quantum Chem.* **1974**, *8*, 61−72.
(36) Engels, B.; Hanrath, M. *DIESEL-MRCI*; Universität Bonn: Germany, 1997.
(37) Dunning, T. H., Jr. *J. Chem. Phys.* **1989**, *90*, 1007−1023.
(38) Widmark, P. O.; Malmqvist, P.; Roos, B. O. *Theor. Chim. Acta* **1990**, *77*, 291−306.
(39) Barone, V.; Cossi, M. *J. Phys. Chem. A* **1998**, *102*, 1995−2001. Barone, V.; Cossi, M. *J. Chem. Phys.* **1998**, *109*, 6246−6254.
(40) Glendening, E. D.; Badenhoop, J. K.; Reed, A. E.; Carpenter, J. E.; Weinhold, F. *NBO*, version 4.0; Theoretical Chemistry Institute, University of Wisconsin: Madison, WI, 1994. Glendening, E. D.; Weinhold, F. *J. Comput. Chem.* **1998**, *19*, 593−609. Glendening, E. D.; Weinhold, F. *J. Comput. Chem.* **1998**, *19*, 610−627. Glendening, E. D.; Badenhoop, J. K.; Weinhold, F. *J. Comput. Chem.* **1998**, *19*, 628−646.

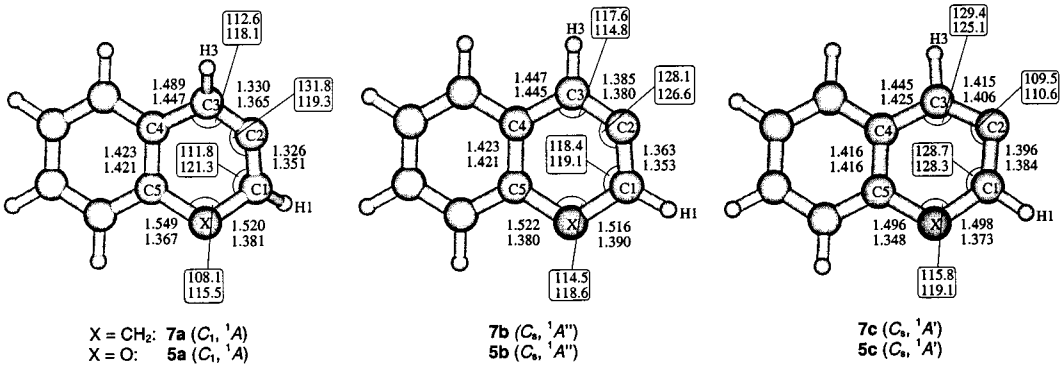

Figure 2. Selected bond lengths (Å) and angles (deg) of various stationary points computed (UB3LYP/cc-pVDZ) for the chromene **5** (lower values) and the isonaphthalene **7** (upper values). Dihedral angles (deg) in **7a**/**5a**: H1−C1−C2−C3, 140.7/163.6; H3−C3−C2−C1, 147.9/158.2; X−C1−C2−C3, −21.6/−16.9; C1−C2−C3−C4, −18.5/−12.8.

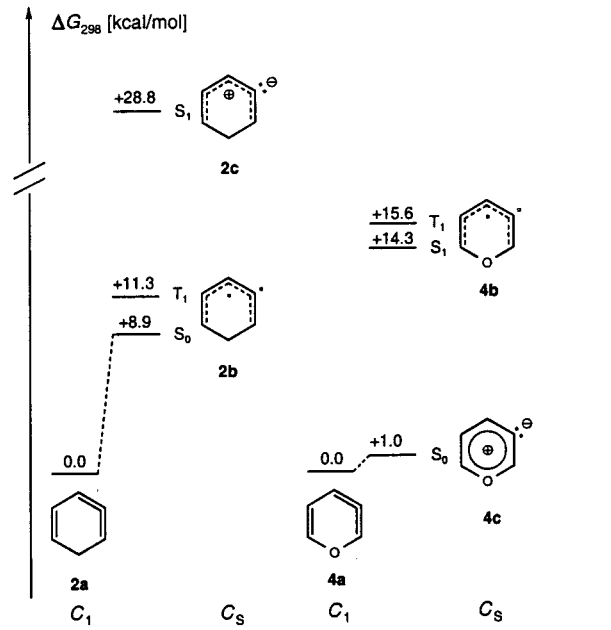

Figure 3. Relative free energies computed (MR-CI+Q/cc-pVDZ//DFT, for the thermal corrections see Computational Details) for various stationary points of the isobenzene **2** and the pyran **4**.

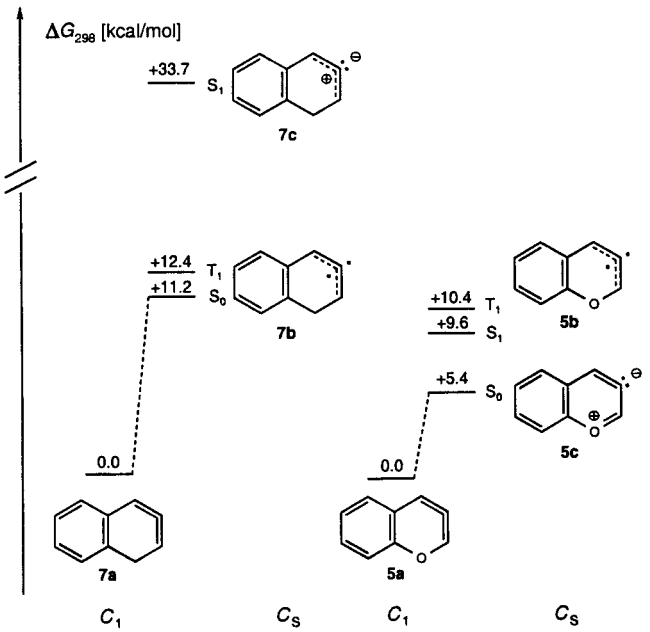

Figure 4. Relative free energies computed (MR-CI+Q/cc-pVDZ//DFT, for the thermal corrections see Computational Details) for various stationary points of the isonaphthalene **7** and the chromene **5**.

C1−C2−C3−H3). The MR-CI expansion (Table 3) reveals that the dominating configuration possesses only doubly occupied orbitals, indicating a closed shell structure of **2a**. As obvious from Figure 5, the HOMO of **2a** is largely localized along the allene moiety. The NRT analysis reveals that the allene resonance structure has the strongly dominating contribution of 69% (Table 2); zwitterionic and diradical resonance structures have only minor contributions of up to 5%. Consequently, both the MR-CI expansion and the NRT analysis indicate that the electronic structure of the ground state of **2** is that of the strained allene **2a**.

Qualitative MO considerations[1] show that the frontier orbitals of the planar structures of cyclic allenes consist of an sp^2-hybridized σ-type orbital and the nonbonding π orbital of an allyl system, which are similar in energy but not entirely equal. Therefore, the planar structure can be classified as a heterosymmetric diradicaloid.[41] From the different occupations of both frontier orbitals, four electronic states can be constructed. Both closed shell structures (σ^2 or π^2 occupation) lead to zwitterionic states, while a triplet and a singlet diradical state result from the occupation pattern $\sigma^1\pi^1$. Within the present C_s symmetry, both zwitterions represent $^1A'$ states, while the diradicals are either of $^1A''$ or $^3A''$ type. The $^1A''$ state (**^{1}2b**) is the lowest lying state for the planar geometry of the isobenzene **2**. This species serves as the transition state (TS) for the racemization of the allene **2a**. Both the MR-CI+Q and the CASPT2 methods compute the energy difference between the TS and the ground state (**2a**) to about 10 kcal/mol (Table 1). This is considerably

Table 1. Relative Electronic Energies (kcal/mol) for Several Stationary Points of the Isobenzene **2** as Calculated by Various Ab Initio Methods: **2a** = Allene, **^{1}2b** = Singlet Diradical, **^{3}2b** = Triplet Diradical, **2c** = Zwitterion

method	2a	^{1}2b	^{3}2b	2c
MR-CI+Q/cc-pVDZ//DFT[a]	0	+10.2	+12.7	+26.5
MR-CI+Q/ANO-l//DFT[a]	0	+9.9	+12.7	+24.9
CASPT2/cc-pVDZ//DFT[a]	0	+10.4	+12.1	+31.3
CASPT2/ANO-l//DFT[a]	0	+9.0	+11.7	+30.4
UCCSD(T)/6-311G(d,p)//DFT[a]	0	+13.2	+14.3	+28.7
MP2/6-311G(d,p)//DFT[a]	0	+27.4	+26.7	+25.5
PUMP2/6-311G(d,p)//DFT[a]	0	−94.5	+17.7	+25.5

[a] UB3LYP/cc-pVDZ.

(41) Bonačić-Koutecký, V.; Koutecký, J.; Michl, J. *Angew. Chem., Int. Ed. Engl.* **1987**, *26*, 170−189.

Table 2. Characterization of the Electronic Structures of Several Stationary Points of the Isobenzene **2** (X = CH_2) and the Pyran **4** (X = O) by Means of the Natural Resonance Theory (NRT) Analysis[a]

stationary point	symmetry state	allene	diradical			zwitterion						Σ
2a	C_1, ^1A	69%	5%	5%						2%		81%
2b	C_s, $^1A''$	—	38%	19%	17%							74%
2c	C_s, $^1A'$	—						33%	23%	10%	5%	71%
4a	C_1, ^1A	21%				7%	9%	13%	4%	3%		57%
4b	C_s, $^1A''$	—	37%	17%	13%							67%
4c	C_s, $^1A'$	—				11%	11%	21%	8%	6%		57%

[a] Blanks denote contributions of less than 2%.

Table 3. Dominating Configurations of the MR-CI Expansions for Several Stationary Points of the Isobenzene **2** and the Pyran **4**

stationary point	symmetry state	configuration	coefficient
2a	C_1, ^1A	$\|(1a)^2...(21a)^2>$	0.885
		$\|(1a)^2...(20a)^2(22a)^2>$	−0.164
2b	C_s, $^1A''$	$\|(1a')^2...(17a')^2\mathbf{(18a')^1}; (1a'')^2...(3a'')^2\mathbf{(4a'')^1}>$	0.903
2c	C_s, $^1A'$	$\|(1a')^2...(18a')^2; (1a'')^2...(3a'')^2>$	0.887
		$\|(1a')^2...(18a')^2; (1a'')^2(2a'')^2(4a'')^2>$	−0.167
		$\|(1a')^2...(18a')^2; (1a'')^2(2a'')^1(3a'')^1(4a'')^1(5a'')^1>$	−0.094
4a	C_1, ^1A	$\|(1a)^2...(21a)^2>$	0.895
		$\|(1a)^2 ...(20a)^2(22a)^2>$	−0.138
4b	C_s, $^1A''$	$\|(1a')^2...(17a')^2\mathbf{(18a')^1}; (1a'')^2...(3a'')^2\mathbf{(4a'')^1}>$	0.901
4c	C_s, $^1A'$	$\|(1a')^2...(18a')^2; (1a'')^2...(3a'')^2>$	0.899
		$\|(1a')^2...(18a')^2; (1a'')^2(2a'')^2(4a'')^2>$	−0.130

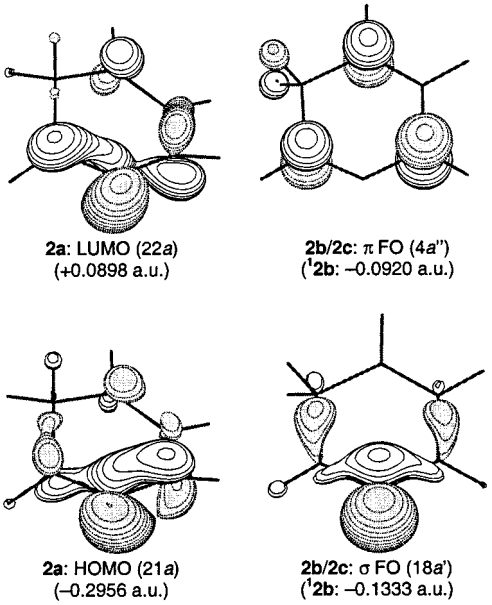

Figure 5. Frontier orbitals (FO) of various stationary points of the isobenzene **2** (energies in atomic units, based on a CASSCF/cc-pVDZ calculation).

higher than the result of the only previous study, which predicted a value of 2 kcal/mol on the basis of a semiempirical treatment (AM1-CI).[14]

While the UCCSD(T) method gives a value in fair agreement with the MR-CI+Q and CASPT2 results (Table 1), the poor performance of MP2 and PUMP2 demonstrates the complexity of the electronic situation in these species. The bond lengths of ^{1}**2b** (Figure 1, X = CH_2) display the characteristic alternation pattern of a pentadienyl radical. Figure 5 depicts the singly occupied molecular orbitals (SOMOs) of ^{1}**2b** (18*a*′ and 4*a*″), demonstrating its σ-π-diradical character. The NRT analysis (Table 2) reveals three important resonance structures, which correspond to the expected σ-π-diradical species. This is in line with the MR-CI expansion (Table 3), which is dominated by the configuration $|(1a')^2...(17a')^2\mathbf{(18a')^1}; (1a'')^2...(3a'')^2\mathbf{(4a'')^1}>$ with a coefficient of 0.903.

Both the MR-CI+Q and the CASPT2 calculations predict the triplet diradical ^{3}**2b** ($^3A''$) to be energetically 12−13 kcal/mol above **2a**, the absolute minimum of **2**. Thus, the triplet state is approximately 2−3 kcal/mol higher in energy than ^{1}**2b**. The value obtained at the UCCSD(T) level is 14.3 kcal/mol above that of **2a**. As expected, the optimized geometry of ^{3}**2b** is planar and virtually identical with that of ^{1}**2b**.

The first excited singlet state of planar **2** is the zwitterion **2c** ($^1A'$). At the MR-CI+Q level, the energy of **2c** is calculated to be 25−27 kcal/mol above that of **2a**, whereas CASPT2 predicts a relative energy of +30−31 kcal/mol. This deviation in the results of these methods is probably due to flaws in the CASSCF-reference wave function, which cannot fully account for mixing with higher lying singlet states of the same symmetry ($^1A'$). The UCCSD(T) calculation for **2c** predicts a relative energy of +28.7 kcal/mol (Table 1). The computed ΔG_{298} values of the electronic states **2a**,**b**,**c** are summarized in Figure 3. The NRT analysis for **2c** (Table 2) reveals three important zwitterionic resonance structures having two electrons in the nonbonding σ orbital and a positively charged π system. The strongly dominating reference configuration of the MR-CI expansion (Table 3) shows the same electronic structure. Representing a local minimum at the S_1 energy surface, zwitterion **2c** exhibits remarkable geometric features (Figure 1), which differ significantly from those of **2a** and **2b**. Most strikingly, the angle C1−C2−C3 is considerably smaller (105.9°) than that of **2a** (130.8) and **2b** (127.8), which originates from the electronic repulsion of the lone pair at C2 and the neighboring C−C bonds.

The relationship between the frontier orbitals of **2a** and those of **2b**/**2c** is illustrated in Figure 5. Obviously, the HOMO (21*a*) and the LUMO (22*a*) of **2a** represent a mixing of the frontier orbitals 18*a*′ and 4*a*″ of the planar structures with rather similar contributions.

To elucidate how the electronic structure of strained cyclic allenes is affected by benzannulation, we performed calculations of the isonaphthalene **7**. Figure 4 summarizes the relative free

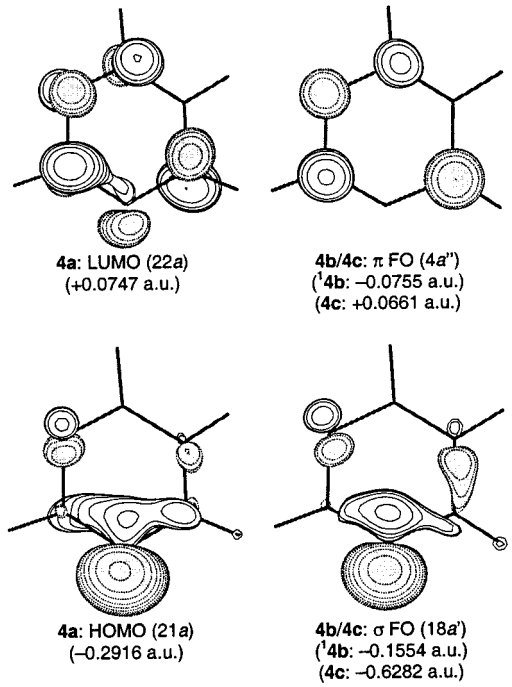

Figure 6. Frontier orbitals (FO) of various stationary points of the pyran **4** (energies in atomic units, based on a CASSCF/cc-pVDZ calculation).

energies ΔG_{298} of the allene (**7a**), the diradical (**7b**), and the zwitterion (**7c**). The optimized geometries are depicted in Figure 2. All these results show that only small differences exist between the isobenzene **2** and isonaphthalene **7**. Relative to the energetics of **2** (Figure 3), **7a** is slightly stabilized with respect to the other species (Figure 4). This result mainly reflects less ring strain imposed on the allene subunit due to the increased length of the bond C4−C5 (1.423 Å vs 1.352 Å in **2a**), which is a consequence of the aromatic delocalization of the corresponding π bond in **7**.

Pyran 4 and Chromene 5. In accordance with the result for **2**, our calculations predict the energy minimum of **4** to possess the C_1-symmetric geometry of **4a** resembling **2a** (Figure 1). However, the dihedral angles at the allene subunit indicate that **4a** (H1−C1−C2−C3, 170.4°; H3−C3−C2−C1, 164.0°; O−C1−C2−C3, −10.9°; C1−C2−C3−C4, −11.2°) is substantially closer to the planar arrangement than is **2a** (H1−C1−C2−C3, 146.4°; H3−C3−C2−C1, 145.8°; C6−C1−C2−C3, −16.2°; C1−C2−C3−C4, −18.2°). Furthermore, a reduced double bond character of the bonds C1−C2 and C2−C3 is apparent from their lengths of 1.362 and 1.394 Å, respectively, as compared with 1.333 and 1.337 Å of **2a**. The most intriguing feature is the bond angle of the allene subunit (C1−C2−C3, 115.6°), which is smaller by 15.2° than that of **2a**. The deviations between the geometrical parameters of **2a** and **4a** result from the differences of their electronic structures, which are revealed by the frontier orbitals (Figure 6) and the NRT analysis (Table 2). The HOMO (21*a*) of **4a** is more strongly localized at C2 than is that of **2a**, indicating some lone-pair character similar to the situation of **2c**. As shown by the NRT analysis, the leading resonance structure is still that having the allene nature (21%), but, in line with the shapes of the frontier orbitals, a series of zwitterionic resonance structures, summing up to a weight of 36%, impose a substantial dipolar character on **4a**. This feature of the ground-state energy minimum of the pyran **4** is in sharp contrast to the situation of the isobenzene **2**. Zwitterionic resonance structures contribute hardly at all to its ground state, whereas diradical ones are of some importance.

At variance with that of **2**, the lowest lying singlet species of planar **4** is the $^1A'$ state, which possesses zwitterionic character (**4c**). Its free energy relative to that of **4a** is calculated to be only +1 kcal/mol (Figure 3). Frequency calculations (UDFT) reveal one imaginary frequency, identifying **4c** as a transition state for the racemization of **4a**. The optimized geometry of **4c** (Figure 1) is very similar to that of **2c**, with the angle C1−C2−C3 being characteristically small (**2c**, 109.5°; **4c**, 110.7°). The singlet diradical **^{1}4b** is calculated to lie 14.3 kcal/mol above **4a** and represents the first excited singlet state (S_1). Frequency calculations characterize **^{1}4b** as an energy minimum. Figure 6 depicts the singly occupied molecular orbitals (SOMOs) of **^{1}4b** (18*a*′ and 4*a*″), which are very similar to their analogues of **2b**. For the corresponding triplet diradical **^{3}4b**, which is a minimum on the T_1 surface, the MR-CI+Q calculation predicts a relative free energy of +15.6 kcal/mol. Both diradicals **4b** have nearly identical geometric parameters. A comparison to the diradical states of **2** reveals no significant differences in the bond lengths and angles (Figure 1). Figure 3 shows that on going from the isobenzene **2** to the pyran **4**, the zwitterionic state ($^1A'$) is strongly stabilized with respect to the diradical states ($^1A''$, $^3A''$). Reasons for this stabilization are offered by both the NRT analysis and the shape of the frontier orbitals. The participation of the oxygen atom opens the possibility of a conjugated π system with six electrons. Indeed, the NRT analysis furnishes two resonance structures of that type. Although they do not make the dominating contributions due to the positive charge at the oxygen center, they stabilize the zwitterionic state in comparison with **2c**, where such aromatic structures are impossible.

The different state order in the planar species of **2** and **4** can also be explained by the differences between their frontier orbitals [σ (18*a*′) and π (4*a*″)]. The π orbital of **4b**,**c** has a strong antibonding (destabilizing) contribution from the oxygen atom. Owing to the methylene group, the antibonding character of this MO of **2** is much smaller. This is mirrored in the σ-π orbital energy differences for the diradicals (**^{1}2b**, 0.0413 au; **^{1}4b**, 0.0799 au). Thus, the single occupation each of the σ and the π orbital in the planar species of **4** is disfavored over the double occupation of the σ orbital, whereas the energetics are reversed for **2**. These situations are commonly referred to as weak (**^{1}2b**) and strong (**^{1}4b**) heterosymmetric diradicaloids.[41]

In summary, our investigations clearly show that on going from the planar structures of **2** to those of **4**, the substitution of the methylene group by an oxygen atom leads to a different energetic order of the electronic states. While in the case of **2** the diradical **^{1}2b** ($^1A''$) represents the lowest singlet state, its place is taken by the zwitterion **4c** ($^1A'$) in the case of **4**. However, the structural parameters within the pairs **2b**/**4b** and **2c**/**4c** do not differ significantly. The variations in the bond lengths X−C1 and X−C5 arise mainly from the different covalent radii of carbon and oxygen. This different state order found for the planar structures explains the increased zwitterionic character of the ground-state minimum of **4** as compared to that of **2**. In analogy to **2a**, the frontier orbitals of **4a** (21*a* and 22*a*) arise from a mixing of the frontier orbitals of the planar species (18*a*′ and 4*a*″). However, in contrast to that of **2a**, the HOMO (21*a*) of **4a** resembles more the 18*a*′ orbital, while the LUMO (22*a*) is more similar to the 4*a*″ orbital (Figure 6), that is, the

Table 4. Solvation Energies (THF) and Relative Energies (kcal/mol) of the Pairs of Stationary Points **4a/4c** and **5a/5c** in Solution as Calculated at the UB3LYP-CPCM/6-31G+(d) Level

	4a	4c	5a	5c
$\Delta\Delta G_{298}^{\text{gas phase}}$	0	+1.0[a]	0	+5.4[b]
$\Delta G_{298}^{\text{solvation}}$	−3.9	−5.1	−2.6	−4.8
$\Delta\Delta G_{298}^{\text{solution}}$	0[c]	−0.2	0	+3.2

[a] From Figure 3. [b] From Figure 4. [c] Not a minimum, fixed geometry.

ground-state minimum of **4** correlates mainly with the lowest lying $^1A'$ state (**4c**) and therefore adopts a substantial zwitterionic character.

The optimized geometries of various stationary points of the chromene **5** are depicted in Figure 2, while the calculated relative free energies are summarized in Figure 4. The zwitterion **5c** is found to lie 5.4 kcal/mol above the allene **5a**, which represents the ground-state energy minimum of **5**. For the chlorochromene **6**, the energy difference between the allene structure **6a** and the zwitterion **6c** has been calculated to be only 2.5 kcal/mol.[4] With **5c** being the transition state for the racemization of **5a**, the barrier to this process is 4.4 kcal/mol higher than that of **4a**. This reflects a reduced ring strain in consequence of the benzannulation as discussed for the energetics of the carbocycles **2** and **7**. However, there is a difference between the carbocyclic (**2**/**7**) and the heterocyclic systems (**4**/**5**). While for **2**/**7** the benzannulation stabilizes the allene structure with respect to all other species, for **4**/**5** only the zwitterionic state is destabilized, whereas both diradical states are significantly stabilized. This stabilization of the diradical states of **5** relative to those of **4** can be rationalized within the formalism of strong and weak hetereosymmetric diradicaloids.[41] The benzannulation decreases the energy gap between the σ and π SOMO (^{1}**4b**, 0.0799 au; ^{1}**5b**, 0.0745 au). For strongly heterosymmetric diradicaloids such as ^{1}**4b** and ^{1}**5b**, this generally results in a stabilization of the diradicaloid with respect to the zwitterionic state.[41] These predictions are mirrored by the calculated MR-CI+Q energies (Figures 3, 4). On the other hand, the results appear to fit the naive picture that **4** has more "aromaticity" to gain from a zwitterionic structure (**4c**) than does **5** in **5c**.

Solvent Effects on 4 and 5. Whereas the above results describe the cyclic allenes **2**, **4**, **5**, and **7** in the gas phase, trapping reactions of them have typically been carried out in solution. Therefore, we have estimated free energies of solvation for the allene and the zwitterionic species of the pyran **4** and the chromene **5** (Table 4), where solvent effects are expected to be more significant than in the case of the less polar compounds **2** and **7**. As anticipated, the zwitterions **4c** and **5c** are more strongly stabilized (5.1 and 4.8 kcal/mol, respectively) than the allene species **4a** and **5a** (3.9 and 2.6 kcal/mol, respectively). In consequence, **4c** represents the energy minimum of **4** in solution, and thus the reacting species preserves no allene character. Owing to the gas-phase energy gap of 5.4 kcal/mol between **5a** and **5c**, the former remains the ground state even in solution, being more stable than **5c** by 3.2 kcal/mol.

Interpretation of the Reactivity of 2, 4, 5, and 7. As cycloadducts with activated olefins were obtained with **5**[20] but not with **4** (see Section 2), it is tempting to ascribe this different reactivity to the different ground states of these intermediates in solution. However, the conclusion that zwitterionic ground states such as **4c** are unable to undergo cycloaddition is unjustified at present, since an activated olefin and the nucleophile KO*t*-Bu compete for the intermediates and the outcome could just be a matter of the relative rates. Tolbert, Houk, et al.[42] have recently presented results of a theoretical study that ascribes a two-step course even to [4 + 2] cycloadditions of cyclohexa-1,2-diene (**1**), with diradicals being the intermediates. Given such a mechanism, it is not obvious from the frontier orbitals of **2a** and **4c** (or **4a**) (Figures 5, 6) which of the two species would attack, for example, furan faster to give an intermediate with a pentadienyl-radical subunit in the six-membered ring and an allyl-radical subunit in the part originating from furan. But Figures 5 and 6 do show a lowering of the LUMO energy as the polar character of the species increases, and hence the rate for the interception by a nucleophile should be higher for the more polar intermediate. Thus, the pyran **4** should be the intermediate most susceptible to the interception by KO*t*-Bu since to the zwitterion **4c** is the ground state or at least very close to it in energy.

A clear-cut conclusion is possible with respect to the site of the attack of a nucleophile. In the case of **2a**, the ground state of the isobenzene **2**, the center with the largest coefficient of the LUMO is the central allene carbon atom (Figure 5). There the attack of a nucleophile should take place. Being much more polar, **4a** has the largest LUMO coefficients at the termini of the allene subunit, and the coefficient at the "central allene" carbon atom is even zero in the LUMO of **4c**. Thus, the calculations are in agreement with the formation of the ether **12** from the pyran **4** and KO*t*-Bu (Scheme 2). Trapping products of **2** with nucleophiles have not been obtained yet, but the experimental findings that the isonaphthalene **7** and the chromene **5** are attacked by KO*t*-Bu at different sites, that is, **7** at the allene center[22] and **5** at the allene terminus bearing the oxygen atom,[20] support the theoretical model outlined for **2** and **4**.

Comparison of the Barriers to Racemization of Six-, Seven-, and Eight-Membered Cyclic Allenes. Previous calculations on cyclohexa-1,2-diene (**1**)[14,43,44] agree with the experimental findings[45] that the ground state has the allene structure **1a**. As the transition state for the racemization, the singlet diradical ^{1}**1b** has been characterized.[14,43] Employing methods as for the calculations of **2**, **4**, **5**, and **7**, we have revisited **1a** and ^{1}**1b**. The structures, optimized at the DFT level of theory, are depicted in Figure 7. The geometric parameters closely resemble those reported by Schleyer at al.[44] At variance with **1a**, ^{1}**1b** has a plane of symmetry, which is perpendicular to the plane of the allyl diradical subunit. Table 5 contains the relative electronic energies and the relative free energies of **1a** and ^{1}**1b** as predicted by the MR-CI+Q and the CASPT2 methods, the results of which differ by 2 kcal/mol. The findings are very similar to the most likely barrier to racemization of ca. 15 kcal/mol suggested by Johnson et al.[43]

In Table 6, we have collected the barriers to racemization of the present work and of three more cyclic allenes, for which theoretical and/or experimental data are available. The difference of ca. 5 kcal between the barriers of **1a** and **2a** nicely reflects the difference between the resonance energies of the allyl and the pentadienyl radical.[46] As anticipated, the barriers increase

(42) Nendel, M.; Tolbert, L. M.; Herring, L. E.; Islam, Md. N.; Houk, K. N. *J. Org. Chem.* **1999**, *64*, 976−983.
(43) Angus, R. O., Jr.; Schmidt, M. W.; Johnson, R. P. *J. Am. Chem. Soc.* **1985**, *107*, 532−537.
(44) Bettinger, H. F.; Schleyer, P. v. R.; Schreiner, P. R.; Schaefer, H. F., III. *J. Org. Chem.* **1997**, *62*, 9267−9275.
(45) Balci, M.; Jones, W. M. *J. Am. Chem. Soc.* **1980**, *102*, 7607−7608.

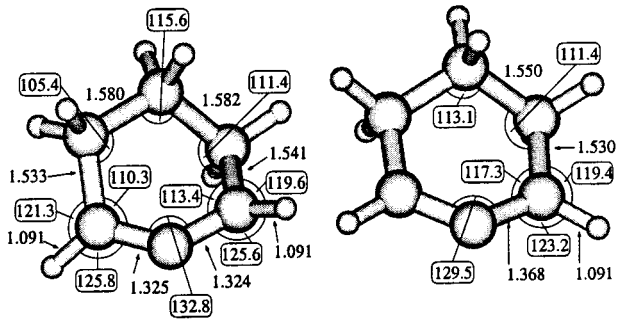

Figure 7. Selected bond lengths (Å) and angles (deg) of cyclohexa-1,2-diene (**1a**) and the transition state for its racemization (^{1}**1b**). Dihedral angles (deg) of the allene subunit in **1a**: H−C−C−C, 143.0; C−C−C−C, −24.6.

Table 5. Relative Electronic Energies (kcal/mol) for Cyclohexa-1,2-diene (**1a**) and the Singlet Diradical ^{1}**1b** as Calculated by Two Ab Initio Methods

method	**1a**	^{1}**1b**[a]
MR-CI+Q/ANO-l//DFT[b]	0	+15.4 (+14.1)
CASPT2/ANO-l//DFT[b]	0	+17.4 (+16.2)

[a] The numbers in parentheses are ΔG_{298} values; for their calculations see Computational Details. [b] UBLYP/6-311G(2d,p).

with ring size. Although the transition state in the case of cyclohepta-1,2,4,6-tetraene (CHT) is stabilized by a conjugated π-electron system, its energy is at least 6 kcal/mol higher than that of **1a**. The $\Delta G^{\ddagger}_{298}$ value for cycloocta-1,2,5-octatriene (COT) was experimentally determined to be 40.6 kcal/mol[49] and is thus astoundingly close to that of unstrained allenes such as 1,3-dimethylallene (44.9 kcal/mol).[50]

5. Heat of Formation of the Isobenzene 2

On the basis of high level quantum chemical calculations, we predict the $\Delta H_f°$ value of **2** to be 75−77 kcal/mol greater than that of benzene. The spread arises from the small deviations between the various approaches.[51] These results nicely agree with the data given by Schleyer et al.[15] (73.7 kcal/mol, CCSD(T)/DZP//B3LYP/DZP + ZPVE) and Rogers et al.[16] (75.1 kcal/mol, G2(MP2)). All theoretical investigations agree that the electronic structure of the ground state of **2** is that of the strained allene **2a**. However, on the basis of an experimental study (see Introduction), Roth et al.[13] deduced a $\Delta H_f°$ value of **2** being 85.3 kcal/mol greater than that of benzene and suggested the diradical ^{1}**2b** to be the ground state of **2**. In this connection, it is worth mentioning that the experimental enthalpy difference between hexa-1,3-dien-5-yne, the starting material of Roth et al.,[13] and benzene (64.9 kcal/mol[52]) is well reproduced by our calculations.[53] Since both hexa-1,3-dien-5-yne and **2a** possess a closed shell electronic structure, a failure of all the theoretical approaches in the case of **2a** is highly unlikely. On the other hand, a solution of the discrepancy between the present results and the conclusion of Roth et al.[13] is important, because a failure of our approach would throw major doubts on all of our findings. Therefore, we checked the key assumptions made in the interpretation of the experimental data. The thermolysis of hexa-1,3-dien-5-yne furnishes benzene,[52,54] but the formation of benzene is suppressed by the presence of $^3O_2$, because the intermediate **2** is trapped by $^3O_2$.[13] By assuming that the latter reaction is controlled by encounter ($k = 2.4 \times 10^9 \exp[0.57/RT]$ M^{-1} s^{-1}), the conversion rates of a number of experiments carried out under different pressures of $^3O_2$ were simulated to give all the rate constants of the kinetic model and, in consequence, the depth of the well for **2** (Figure 8).

Now, the assumption of encounter control for the interception of **2** by $^3O_2$ is justified only if the intermediate has the character of a diradical, that is, that of **2b**. Doubtless, the reaction will be slower in the case of a closed-shell nature of the intermediate such as **2a**.[55] Therefore, we have tried to numerically simulate[56] the experimental data[13] presupposing a smaller rate constant than that of encounter control. Indeed, a satisfactory agreement was obtained with $k = 6 \times 10^6 \exp[0.57 - 7/RT]$ M^{-1} s^{-1}, giving rise to a $\Delta H_f°$ value for **2** that is 78 kcal/mol above that of benzene (Figure 8) and only 1−3 kcal/mol above our calculated values. The preexponential factor of 6×10^6 M^{-1} s^{-1} is not unreasonable for a gas-phase reaction.[57]

By imposing encounter control on the trapping of **2** by $^3O_2$, Roth et al.[13] obviously determined the upper limit for $\Delta H_f°$ of **2** (85.3 kcal/mol above benzene). A very similar value (86.5 kcal/mol above benzene) was estimated for the diradical **2b** by these authors using group equivalents. According to our calculations, ^{1}**2b** is the transition state for the enantiomerization of **2a** with an energy lying 85−87 kcal/mol above that of benzene. Therefore, the experiment and the theory virtually coincide as to the energetics of diradical **2b**, whereas at present a rather reliable $\Delta H_f°$ value for **2a** is accessible only by calculations.

6. Experimental Section

General Methods. See ref 22.

4*H*-Pyran (8). Crude **8** was prepared as described in ref 58 and was used in the next step without purification. The content of pure **8** was determined by ^{1}H NMR spectroscopy using an internal standard. ^{1}H NMR (200 MHz, $CDCl_3$): δ 2.72 (tt, 2H, $J_{3,4} = +3.3$, $J_{2,4} = -1.8$ Hz; H4), AA′MM′ part of an AA′MM′X_2 spectrum at 4.75 (2H, H3, H5) and 6.25 (2H, H2, H6) with $J_{2,3} = +6.3$, $J_{2,4} = -1.8$, $J_{2,5} = +0.7$, $J_{2,6} = +0.6$, $J_{3,4} = +3.3$, $J_{3,5} = +2.5$ Hz. The values of the coupling constants were supported by simulation of the spectrum, and the assignment of $J_{2,6}$ and $J_{3,5}$ is based on the value of $J_{2,6}$ of **9** (unresolved). ^{13}C NMR (63 MHz, $CDCl_3$): δ 18.5 (C4), 100.9 (C3, C5), 140.7 (C2, C5).

(46) Roth, W. R.; Staemmler, V.; Neumann, M.; Schmuck, C. *Liebigs Ann. Chem.* **1995**, 1061−1118.
(47) Schreiner, P. R.; Karney, W. L.; Schleyer, P. v. R.; Borden, W. T.; Hamilton, T. P.; Schaefer, H. F., III. *J. Org. Chem.* **1996**, *61*, 7030−7039.
(48) Warmuth, R. *J. Am. Chem. Soc.* **2001**, *123*, 6955−6956.
(49) Roth, W. R.; Bastigkeit, T. *Liebigs Ann. Chem.* **1996**, 2171−2183.
(50) Roth, W. R.; Ruf, G.; Ford, P. W. *Chem. Ber.* **1974**, *107*, 48−52.
(51) MR-CI+Q/ANO-l[5s3p1d/3s1p], 77.0 kcal/mol; CASPT2/ANO-l, 75.7 kcal/mol; CCSD(T)/6-311G (2d), 75.8 kcal/mol; geometry optimizations and thermal corrections to the relative enthalpy (ΔH_{298}) on the UB3LYP/6-311G(2df,p) level of theory.
(52) Roth, W. R.; Hopf, H.; Horn, C. *Chem. Ber.* **1994**, *127*, 1781−1795.
(53) CCSD(T)/6-311G (2d), 65.0 kcal/mol (geometry optimizations and thermal corrections to the relative enthalpy (ΔH_{298}) on the UB3LYP/6-311G(2df,p) level of theory); G2(MP2), 65.6 kcal/mol.
(54) Hopf, H.; Musso, H. *Angew. Chem., Int. Ed. Engl.* **1969**, *8*, 680.
(55) For the reaction of $^3O_2$ with activated olefins, see: Ingold, K. U. *Acc. Chem. Res.* **1969**, *2*, 1−9.
(56) The simulations were carried out using the LSODAR package: Hindmarsh, A. C. In *Scientific Computing*; Stepleman, R. S., Vitchnevetsky, R., Eds.; North-Holland: Amsterdam, 1983; pp 55−64.
(57) Moore, J. W.; Frost, R. G. *Kinetics and Mechanism; A Study of Homogeneous Chemical Reactions*, 3rd ed.; Wiley: New York, 1981; p 197.
(58) Strating, J.; Keijer, J. H.; Molenaar, E.; Brandsma, L. *Angew. Chem.* **1962**, *74*, 465. Lürken, W.; Müller, E. *Methoden Org. Chem.* (*Houben-Weyl*), *4th ed.* **1966**, *VI/4*, 100−110.

Table 6. Barriers to Racemization (kcal/mol) of Six-, Seven-, and Eight-Membered Cyclic Allenes in the Gas Phase

allene			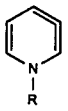		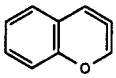	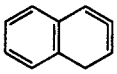		
	1a	**2a**	**3a**	**4a**	**5a**	**7a**	**CHT**	**COT**
$\Delta G^{\ddagger}_{298}$, calcd	14.1[a]	8.9[a]	0[b]	1.0[a]	5.4[a]	11.2[a]	20[c]	
$\Delta G^{\ddagger}_{298}$, exptl	[d]						21.7[e]	40.6[f]

[a] This work; values from Table 5 and Figures 3 and 4. [b] Reference 17a. [c] Activation energy: ref 47. [d] The chirality of **1a** and the rather ready racemization has been demonstrated: ref 45. [e] Estimated from the kinetic data determined for 5-methylcyclohepta-1,2,4,6-tetraene, which was incarcerated in a molecular container: ref 48. [f] $\Delta H^{\ddagger}$= 39.8 kcal/mol, $\Delta S^{\ddagger}$= −2.8 e.u.: ref 49.

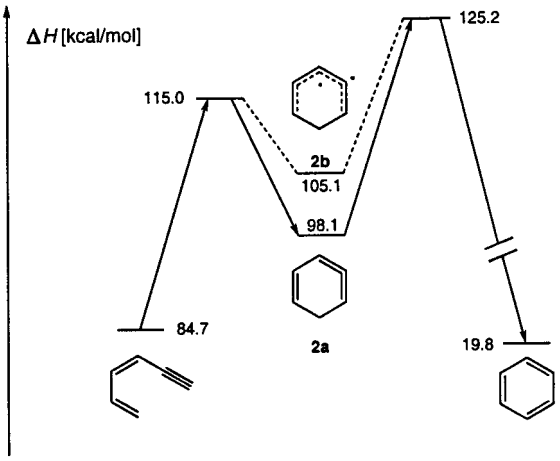

Figure 8. Energy profile for the thermal rearrangement of hexa-1,3-diene-5-yne to benzene via the isobenzene **2**. The depth of the well for **2** is accessible by running the kinetics in the presence of $^3O_2$ (ref 13) and estimating a rate constant for the trapping of **2** by $^3O_2$. Roth et al. (ref 13) assumed encounter control and arrived at ΔH_f° = 105.1 kcal/mol for **2**, which supported its diradical nature (**2b**). Herein we show that the assumption of a barrier of 7 kcal/mol to the reaction with $^3O_2$ gives also a satisfactory reproduction of the rate data, leading to ΔH_f° = 98.1 kcal/mol for **2**, which is consistent with its closed shell nature (**2a**) and in line with the result of the present calculations.

2α,3*β*,5α,6*β*-Tetrabromotetrahydropyran (10). Under nitrogen, crude **8** (2.7 mmol) was diluted with anhydrous CH_2Cl_2 to give a solution of 20 mL. Cooled to −78 °C, this solution was stirred and treated dropwise with a solution of Br_2 in CH_2Cl_2 (0.1 M) until the color of Br_2 persisted. The mixture was then concentrated in vacuo. After warming of the solid residue with $Me_3C-O-Me$ (5 mL) to 50 °C, CH_2Cl_2 was added to the suspension to the point at which a solution resulted. The open flask was left at room temperature for 2 days to give **10** (681 mg, 63%) as colorless crystals with mp 132−133 °C. The examination of the mother liquor provided no evidence for a diastereomer of **10**. This procedure was successfully conducted up to 10-fold scale. IR (KBr): 3010, 2990, 2980, 2940, 2920, 1430, 1335, 1280, 1245, 1180, 1160, 1115, 1090, 1040, 980, 940, 925, 880, 830, 745, 735, 675 cm^{-1}. ^1H NMR (250 MHz, $CDCl_3$, ambient temperature): δ 2.92 (t, 2H, line distance 5.7 Hz, H4), 4.57 (q, 2H, line distance 5.6 Hz, H3, H5), 6.24 (d, 2H, line distance 5.5 Hz, H2, H6). ^1H NMR (200 MHz, CD_2Cl_2, −70 °C) δ 2.75 (br d, 1H, ^2J = 14 Hz, $H4_{eq}$), 3.10 (br t, 1H, average of ^2J and ^3J = 13 Hz, $H4_{ax}$), 4.5−4.7 (m, 2H, H3, H5), 5.95 (br d, 1H, J = 9 Hz, $H2_{ax}$), 6.50 (br s, 1H, $H6_{eq}$). ^{13}C NMR (50 MHz, $CDCl_3$, ambient temperature): δ 37.7 (C4), 47.5 (C3, C5), 83.0 (C2, C6). ^{13}C NMR (63 MHz, CD_2Cl_2, −70 °C): δ 36.5 (C4), 46.5, 48.2 (C3, C5), 80.2, 85.3 (C2, C6). Anal. Calcd for $C_5H_6Br_4O$: C, 14.95; H, 1.51. Found: C, 15.36; H, 1.47.

3-Bromo-4*H*-pyran (9). A. From 8 and 1 Equiv of Bromine. Under nitrogen, crude **8** (containing 200 mmol of pure **8**) was diluted with anhydrous CH_2Cl_2 to give a solution of 100 mL. Under stirring and cooling to −78 °C, this solution was treated dropwise with a solution of Br_2 (32.0 g, 200 mmol) in CH_2Cl_2 (40 mL) within 40 min. Freshly distilled $PhNEt_2$ (29.8 g, 200 mmol) was immediately added to the resulting mixture, and CH_2Cl_2 was removed in a rotary evaporator. Under nitrogen, the residue was quickly heated to 100−110 °C (temperature of the oil bath) and kept at that temperature for 10 min. Still kept at 100−110 °C, the flask was connected to a distillation apparatus, and the pressure in the apparatus was slowly reduced to 20−30 mbar, whereby a liquid distilled, which was collected in a cooled receiver (−78 °C). This liquid was shown by NMR spectroscopy to contain $PhNEt_2$ and **8** in addition to **9**. Distillation of this liquid by using a Vigreux column (20 cm) gave pure **9** (3.56 g, 11%) as a yellowish liquid, which turned black at room temperature within several hours: bp 35−40 °C/10−13 mbar. ^1H NMR (250 MHz, $CDCl_3$): δ 3.04 (dt, 2H, $J_{4,5}$ = 3.4, $J_{2,4}$ = $J_{4,6}$ = 1.8 Hz, H4), 4.77 (dt, 1H, $J_{5,6}$ = 6.1, $J_{4,5}$ = 3.4 Hz, H5), 6.29 (dt, 1H, $J_{5,6}$ = 6.1, $J_{4,6}$ = 1.8 Hz, H6), 6.57 (t, 1H, $J_{2,4}$ = 1.8 Hz, H2). ^{13}C NMR (63 MHz, $CDCl_3$): δ 28.7 (C4), 100.4 (C5), 101.3 (C3), 139.56 (C2), 139.61 (C6). The assignment is based on a C,H COSY spectrum. MS (EI, 70 eV) (*m*/*z*): 162 (28%) and 160 (28) [M^+], 161 (100), 159 (91). HRMS (*m*/*z*): calcd for $C_5H_5{}^{79}BrO$ [M^+] 159.9524, found 159.9524.

B. From 10. Under nitrogen, a stirred mixture of **10** (5.00 g, 12.4 mmol) and $PhNEt_2$ (7.88 g, 52.8 mmol) was heated to 200 °C (temperature of the oil bath) within 15−20 min, kept at 200 °C for 5 min, and was then allowed to cool. The flask was equipped with a Vigreux column (20 cm) and a distillation apparatus, and, when the oil bath had reached 110 °C, the volatile components were distilled off in a vacuum of 8−10 mbar. When the receiver was cooled with liquid N_2, the distillate contained **8** and **9** in a ratio of 2:3 in addition to $PhNEt_2$ as shown by NMR spectroscopy. In another experiment, the receiver was cooled with ice, whereby 600 mg of a 2.5:1 mixture of **9** and $PhNEt_2$ were obtained as a yellowish liquid with bp 40−55 °C/8−10 mbar. A careful short-path distillation of this mixture gave rather pure **9** (378 mg, 19%).

3,5-Dibromo-4*H*-pyran (11). Under nitrogen, a solution of **10** (5.50 g, 13.7 mmol) and freshly distilled DBU (8 mL, 53.5 mmol) in anhydrous THF (100 mL) was stirred at room temperature for 20 h. The brown precipitate formed was removed by filtration and washed with THF (2 × 30 mL). The filtrate was concentrated in vacuo to dryness. In a short-path distillation, rather pure **11** (11 mg, 0.3%) was obtained from the residue: bp 100 °C (bath)/10^{-3} mbar. ^1H NMR (250 MHz, $CDCl_3$): δ 3.37 (t, 2H, J = 1.7 Hz, H4), 6.63 (t, 2H, J = 1.7 Hz, H2, H6). ^{13}C NMR (63 MHz, $CDCl_3$): δ 37.5 (C4), 99.0 (C3, C5), 138.5 (C2, C6). MS (EI, 70 eV) (*m*/*z*): 242 (31%), 240 (64), 238 (32) [M^+], 241 (52), 239 (100), 237 (50). HRMS (*m*/*z*): calcd for $C_5H_4{}^{79}Br_2O$ [M^+] 237.8629, found 237.8625.

***tert*-Butyl 4*H*-Pyran-4-yl Ether (12). A. Preparation in Styrene.** Under nitrogen, **9** (171 mg, 1.06 mmol) was added in several portions to a stirred mixture of KO*t*-Bu (230 mg, 2.05 mmol) and 18-crown-6 (280 mg, 1.06 mmol) in styrene (5 mL) at room temperature within 5 min, whereby the mixture adopted a dark color. After continued stirring for 30 min, the volatile components were evaporated at room temperature/10^{-2} mbar and condensed in a cooled receiver. The liquid obtained was shown by NMR spectroscopy to consist mainly of **12**, 18-crown-6, and styrene in a ratio of 1.6:1:20. Attempts to isolate **12** were unsuccessful. ^{1}H NMR (250 MHz, $CDCl_3$): δ 1.23 (s, 9H, 3 CH_3), 4.52 (br tt, $J_{3,4} = +4.0$, $J_{2,4} = -0.7$ Hz, H4), AA′MM′ part of an AA′MM′X spectrum at 5.01 (2H, H3, H5) and 6.60 (2H, H2, H6) with $J_{2,3} = +6.2$, $J_{2,4} = -0.7$, $J_{2,5} = +0.5$, $J_{2,6} = +0.7$, $J_{3,4} = +4.0$, $J_{3,5} = +2.7$ Hz. The values of the coupling constants were supported by simulation of the spectrum, and the assignment of $J_{2,6}$ and $J_{3,5}$ is based on the magnitude of $J_{2,6}$ of **9**. ^{13}C NMR (63 MHz, $CDCl_3$): δ 28.5 (CH_3), 56.4 (C4), 104.8 (C3, C5), 142.0 (C2, C6). The signal of the quaternary atom of the *t*-Bu group was not observed due to low intensity.

B. Preparation in Furan. The reaction was conducted as above, but in furan (3 mL) as solvent instead of styrene. The solvent was removed at room temperature/10 mbar, and the residue was treated with hexane (20 mL). The hexane solution obtained by filtration was concentrated to dryness at room temperature/10 mbar. As shown by ^{1}H NMR spectroscopy, the residue contained **9** and **12** in a ratio of 1.3:1 in addition to 18-crown-6, furan, and several impurities. HRMS of **12** (EI, 70 eV) (*m*/*z*): calcd for $C_9H_{14}O_2$ [M^+] 154.0994, found 154.0995.

C. Preparation in C_6D_6. The reaction was conducted as above, but the solvent was C_6D_6 (3 mL) instead of styrene or furan. After 1 h of stirring at room temperature, the volatile components were evaporated at room temperature/10^{-3} mbar and condensed in a cooled receiver. The C_6D_6 solution obtained was shown by ^{1}H NMR spectroscopy to contain **9** and **12** in a ratio of 2:1, 18-crown-6, and three aldehydes [δ = 9.66 (br s), 9.58 (d, J = 7.7 Hz), and 9.46 (d, J = 9.5 Hz)] in a ratio of 4:1:3, the total amount of which was 95% of that of **12**. By using an internal standard, the yield of **12** was determined to be 7.5% with regard to consumed **9**. We consider this yield as a lower limit as some **12** might have remained in the residue. The amount of 18-crown-6 in the condensate (44% of the starting quantity) is evidence for an incomplete evaporation.

Acknowledgment. This work was supported by the Deutsche Forschungsgemeinschaft and the Fonds der Chemischen Industrie.

Supporting Information Available: Cartesian coordinates and calculated energies for **1a**,**b**, **2a**−**c**, **4a**−**c**, **5a**−**c**, and **7a**−**c** in the gas phase as well as **4a**,**c** and **5a**,**c** in solution (22 tables), NMR spectra of **12**, and a description of the simulation of the experimental rate data with respect to the new ΔH_f° value of **2** (PDF). This material is available free of charge via the Internet at http://pubs.acs.org.

JA011227C